Octopaminergic agonists for the cockroach neuronal octopamine receptor

Authors: Hirashima, Akinori, Morimoto, Masako, Kuwano, Eiichi, and Eto, Morifusa

Source: Journal of Insect Science, 3(10) : 1-9

Published By: Entomological Society of America

URL: https://doi.org/10.1673/031.003.1001

Hirashima A, Morimoto M, Kuwano E, Eto M. 2003. Octopaminergic agonists for the cockroach neuronal octopamine receptor. 9pp. *Journal of Insect Science*, 3:10, Available online: insectscience.org/3.10

Journal of Insect Science

insectscience.org

Octopaminergic agonists for the cockroach neuronal octopamine receptor

Akinori Hirashima[1], Masako Morimoto[2], Eiichi Kuwano[1] and Morifusa Eto[3]

[1]Department of Applied Genetics and Pest Management, Faculty of Agriculture, Graduate School, Kyushu University, Fukuoka 812-8581, Japan.

[2]Department of Bioresource and Bioenvironmental Sciences, School of Agriculture, Kyushu University, 6-10-1 Hakozaki, Higashi-ku, Fukuoka 812-8581, Japan

[3]Professor Emeritus of Kyushu University,7-32-2 Aoba, Higashi-ku, Fukuoka 813-0025, Japan

ahirasim@agr.kyushu-u.ac.jp

Received 14 February 2003, Accepted 13 April 2003, Published 21 April 2003

Abstract

The compounds 1-(2,6-diethylphenyl)imidazolidine-2-thione and 2-(2,6-diethylphenyl)imidazolidine showed the almost same activity as octopamine in stimulating adenylate cyclase of cockroach thoracic nervous system among 70 octopamine agonists, suggesting that only these compounds are full octopamine agonists and other compounds are partial octopamine agonists. The quantitative structure-activity relationship of a set of 22 octopamine agonists against receptor 2 in cockroach nervous tissue, was analyzed using receptor surface modeling. Three-dimensional energetics descriptors were calculated from receptor surface model/ligand interaction and these three-dimensional descriptors were used in quantitative structure-activity relationship analysis. A receptor surface model was generated using some subset of the most active structures and the results provided useful information in the characterization and differentiation of octopaminergic receptor.

Keywords: Periplaneta americana, receptor surface model, cerius2, octopamine agonist

Abbreviation:

AEA	arylethanolamine
AII	2-(arylimino)imidazolidine
AIO	2-(arylimino)oxazolidine
AIT	2-(arylimino)thiazolidine
APAT	2-(α-phenylethylamino)-2-thiazoline
BPAT	2-(β-phenylethylamino)-2-thiazoline
CAO	2-(3-chlorobenzylamino)-2-oxazoline
DCAO	2-(3,5-dichlorobenzylamino)-2-oxazoline
DET5	2-(2,6-diethylphenylimino)-5-methylthiazolidine
DET6	2-(2,6-diethylphenylimino)thiazine
EGTA	ethylene glycol bis(β-aminoethyl ether)-*N*,*N*,*N'*,*N'*-tetraacetic acid
GFA	genetic function approximation
G/PLS	genetic partial least squares
IND	2-aminomethyl-2-indanol
LAH	lithium aluminum hydride
MCSG	maximum common subgroup
MCT6	2-(2-methyl-4-chlorophenylimino)thiazine
OA	octopamine
PLS	partial least squares
QSAR	quantitative structure-activity relationship
SBAT	2-(substituted benzylamino)-2-thiazoline

Abbreviations continued on next page

Abbreviations continued from previous page

SD	the sum of squared deviations of the dependent variable values from their mean
SPIT	3-(substituted phenyl)imidazolidine-2-thione
THI	2-amino-1-(2-thiazoyl)ethanol
TMS	tetramethyl silane

Introduction

Octopamine [2-amino-1-(4-hydroxyphenyl)ethanol] which has been found to be present in high concentrations in various insect tissues, is the monohydroxyllic analogue of the vertebrate hormone noradrenalin. Octopamine was first discovered in the salivary glands of the octopus by Erspamer and Boretti (1951). It has been found that octopamine is present at a high concentrations in various invertebrate tissues (Axelrod and Saavedra, 1977). This multifunctional and naturally occurring biogenic amine has been well studied and established as 1) a neurotransmitter, controlling the firefly light organ and endocrine gland activity in other insects; 2) a neurohormone, inducing mobilization of lipids and carbohydrates; 3) a neuromodulator, acting peripherally on muscles, fat body, corpora cardiaca and the corpora allata, and 4) a centrally acting neuromodulator, influencing motor patterns, habituation and even memory in various invertebrate species (Evans, 1985, 1993). The action of octopamine is mediated through various receptor classes. Three different receptor classes OAR1, OAR2A and OAR2B have been distinguished from non-neuronal tissues (Evans, 1981). OAR2 is coupled to G-proteins and is specifically linked to an adenylate cyclase. Thus, the physiological actions of OAR2 have been shown to be associated with elevated levels of cAMP (Nathanson, 1985). In the nervous system of the locust, *Locusta migratoria*, a particular receptor class was characterized and established as a new class OAR3 by pharmacological investigations of the [^{3}H]OA binding site using various agonists and antagonists (Roeder, 1990, 1992, 1995; Roeder and Gewecke, 1990; Roeder and Nathanson, 1993).

Recently much attention has been directed at the octopamine agonist as a valid target in the development of safer and selective pesticides (Jennings *et al*., 1988; Hirashima *et al*., 1992; Ismail *et al*., 1996). Structure-activity studies of various types of octopamine agonists and antagonists were also reported using the nervous tissue of the migratory locust, *L. migratoria* (Roeder, 1990, 1992, 1995; Roeder and Gewecke, 1990; Roeder and Nathanson, 1993). However, information on the structural requirements of these octopamine agonists and antagonists for high octopamine-receptor ligands is still limited. It is therefore of critical importance to provide information on the pharmacological properties of octopamine receptor types and subtypes. Our interest in octopaminergic agonists was aroused by the results of quantitative structure-activity relationship (QSAR) studies using various physicochemical parameters as descriptors (Hirashima *et al*., 1999a; Pan *et al*., 1997a) and receptor surface modeling (Hirashima *et al*., 1998a). Furthermore, molecular modeling and conformational analyses were performed in Catalyst/Hypo to gain a better understanding of the interactions between octopaminergic antagonists and OAR3 in order to determine the conformations required for binding activity (Pan *et al*., 1997b). A similar procedure was repeated using octopamine agonists (Hirashima *et al*., 1999b). However, binding activity is not enough for evaluating octopamine-agonist activity, because it is difficult to determine the different activities of octopamine agonists and antagonists. In drug discovery, it is common to have measured activity data for a set of compounds acting upon a particular protein but not to have knowledge of the three-dimensional structure of the protein active site. In the absence of such three-dimensional information, one can attempt to build a hypothetical model of the receptor site that can provide insight about receptor site characteristics. Such a model is known as a receptor surface model, which provides compact and quantitative descriptors that capture three-dimensional information about a putative receptor site. Thus, the current work is aimed to perform 3D receptor surface modeling on a set of octopamine agonists using the thoracic nervous system of the American cockroach, *Periplaneta americana*, in which octopamine-agonist action is thought to be due to cAMP elevation at OAR2 (Hirashima *et al*., 1992).

Materials and Methods

Synthesis of OA agonists

AEAs **1-7**, IND **39** and THI **40** were synthesized from trimethylsilyl cyanide and the corresponding aldehyde in the presence of catalytic amount of anhydrous zinc iodide, followed by reduction with LAH (Hirashima *et al*., 1990). AEAs **23** and **24** were obtained by reducing optically active mandelic amides, which was obtained from optically active manelic acids via their esters, with LAH (Wu *et al*., 1989). AITs **9**-**11**, **41-43**, MCT6 **44**, DET5 **45**, DET6 **46**, SBATs **12**-**14**, **47**-**57**, APATs **58**-**59** and BPAT **60** were synthesized by cyclization of the corresponding thiourea with conc. hydrogen chloride (Hirashima *et al*., 1994). AIOs **15**-**16**, **61**-**65**, CAO **17** and DCAO **66** were obtained by cyclodesulfurizing the corresponding thiourea with yellow mercuric oxide (Hirashima *et al*., 1996). SPITs **18** and **67**-**70** were synthesized by the cyclization of monoethanolamine hydrogen sulfate with arylisothiocyanate in the presence of sodium hydroxide as described in the previous report (Hirashima *et al*., 1998b). AIIs **19**-**22** were prepared according to a reported method by refluxing the corresponding substituted aniline and 1-acetyl-2-imidazolidone in phosphoryl chloride followed by hydrolysis (Nathanson and Kaugars, 1989). The structures of the compounds were confirmed by ^{1}H and ^{13}C NMR measured with a JEOL JNM-EX400 spectrometer at 400 MHz, TMS being used as an internal standard for ^{1}H NMR and elemental analytical data.

Chemicals

Octopamine, theophylline (1,3-dimethylxanthine), tyramine **41** and EGTA were purchased from Nacalai Tesque, www.nacalai.co.jp/en/; GTP and DL-synephrine **8** was from Sigma Chemical Co., www.sigmaaldrich.com; ATP disodium salt was from Kohjin Co., www.kohjin.co.jp/english/; LAH was from Chemetall GmbH, www.chemetall.com. The cAMP radioimmunoassay kit (cord RPA 509) was purchased from Amersham International,

www.apbiotech.com.

Insect culture

Males and females of *Periplaneta americana* were used indiscriminately, as their nervous systems exhibited no gross structural or neurochemical differences. The insects were reared under crowded conditions in this laboratory at 28 °C with a photoperiod of 12 h light:12 h dark and at a relative humidity of 65-70% for more than 7 years. They were provided with an artificial mouse diet (Oriental Yeast Co., Chiba, Japan, www.oyc.co.jp/e/) and water *ad libitum*.

Adenylate-cyclase assay

The adenylate-cyclase assay was conducted on adult *P. americana* as described previously (Hirashima *et al*., 1992, 1994, 1996, 1998b). Thoracic nerve cords of *P. americana* were homogenized (15 mg/ml) in a 6 mM Tris-maleate buffer (pH 7.4) using a chilled microtube homogenizer (S-203, Ikeda Sci., Tokyo, Japan, www.biorobotics.com/Pages/ikeda.html) as described previously. The homogenate was diluted (1 mg/ml) in 6 mM Tris-maleate, centrifuged at 120,000 g at 4 °C for 20 min. The supernatant was discarded, the pellet was resuspended by homogenizing (1 mg/ml) in the buffer, and again centrifuged at 120,000 g at 4 °C for 20 min. The resulting pellet (P2) resuspended in the buffer was equivalent to the starting amount (15 mg/ml). The adenylate-cyclase activity was measured according to Nathanson's procedure under optimal conditions (Hirashima *et al*., 1992, 1994, 1996, 1998b) in a test tube containing 200 µl of 120 mM Tris-maleate (pH 7.4, including 15 mM theophylline, 12 mM $MgCl_2$ and 0.75 mM EGTA), 60 µl of the P2 fraction and 30 µl of each synthesized compound solution in polyethylene glycol. An appropriate solvent control was run in parallel. The enzyme reaction (5 min at 30°C) was initiated by adding 10 µl of a mixture of 3 mM GTP and 60 mM ATP, stopped by heating at 90 °C for 2 min and then centrifuged at 1000 g for 15 min to remove the insoluble material. The cAMP level in the supernatant was measured using a radioimmunoassay (Hirashima *et al*., 1992, 1994, 1996, 1998b). Protein concentration was determined by the Lowry method (Lowry *et al*., 1951), using bovine serum albumin (Sigma) as the standard. Enzyme activity in each assay was corrected using octopamine as a reference. The Vmax values (mostly at 0.1 mM) were calculated relative to octopamine (100%) and control (0%).

Computational details

Molecular alignment: All experiments were conducted with Cerius2 3.8 QSAR environment from Accelrys, www.accelrys.com, on a Silicon Graphics O2, runnning under the IRIX 6.5 operating system. Multiple conformations of each molecule were generated using the Boltzmann Jump as a conformational search method. The upper limit of the number of conformations per molecule was 150. Each conformer was subjected to an energy minimization procedure to generate the lowest energy conformation for each structure. Alignment of structures through pair-wise superpositioning placed all structures in the study compounds in the same frame of reference as the shape reference compounds, which were selected as a conformer of the most active octopamine agonists. The method used for performing the alignment was MCSG. This method looks at molecules as points and lines, and uses the techniques of graph theory to identify patterns. It finds the largest subset of atoms in the shape reference compound that is shared by all the structures in the study table and uses this subset for alignment. A rigid fit of atom pairings was performed to superimpose each structure so that it overlays the shape reference compound.

Receptor surface modeling: Receptor surface models are predictive and sufficiently reliable to guide the chemist in the design of novel compounds. These descriptors are used for predictive QSAR (quantitative structure-activity relationship) models. This approach is effective for the analysis of data sets where activity information is available but the structure of the receptor site is unknown. Receptor surface modeling attempts to postulate and represent the essential features of a receptor site from the aligned common features of the molecules that bind to it. This method generates multiple models that can be checked easily for validity. Once a reasonable receptor surface model has been defined, a series of structures can be evaluated against the model. When a receptor model has been generated and the models have been aligned, a QSAR can be built using data from the receptor-structure interactions. The results of the minimization procedure were used as descriptors either to refine the model or to predict activity. Three-dimensional energetics descriptors were calculated from receptor surface model/ligand interaction. These three-dimensional descriptors were used in QSAR analysis.

A receptor surface model represents the global volume that can accommodate one or more molecules and can be seen as the shape of an active site built from the ligands that fit into it in their "active" conformation. The descriptors used in this study account for phenomena that occur at the contact surface between the ligands and the protein active site. A receptor surface model represents essential information about the hypothetical receptor site as a three-dimensional surface with associated properties mapped onto the surface model. The location and shape of the surface represent information about the steric nature of the receptor site: the associated properties represent other information of interest, such as hydrophobicity, partial charge, electrostatic potential and hydrogen-bonding propensity. The isosurface procedure produces a surface that entirely encloses the molecules over which it is generated. The surface has no holes and is known as a closed model. Receptor surface models are best constructed from a set of the most active analogues that are chosen to cover the variety of steric and electrostatic variations likely to appear in the test data. The approach we took was to automatically build a set of different receptor surface models from different combinations of the most active analogues, and then use a variable-selection technique such as G/PLS to discover the receptor surface model whose descriptors yield the best QSARs of the full training set. G/PLS allows the discovery and use of nonlinear descriptors by using spline-based terms.

Genetic partial least squares: Due to the large number of points used as independent variables, genetic partial least squares (G/PLS) was used to derive the QSAR models. G/PLS, a variation of genetic function approximation (GFA), can be run as an alternative to the standard GFA algorithm. G/PLS is derived from the best

features of two methods: GFA and partial least squares (PLS). Both GFA and PLS have been shown to be valuable analysis tools in cases where the data set has more descriptors than samples. In PLS, variables might be overlooked during interpretation or in designing the next experiment even though cumulatively they are very important. This phenomenon is known as "loading spread". In GFA, equation models have a randomly chosen proper subset of the independent variables. As a result of multiple linear regression on each model, the best ones become the next generation and two of them produce an offspring. This was repeated 10000 (default 5000) times. For other settings, all defaults were used. Loading spread does not occur because at most one of a set of co-linear variables is retained in each model. G/PLS combines the best features of GFA and PLS (Cerius2 tutorial. Accelrys Inc., www.accelrys.com/cerius2). G/PLS retains the ease of interpretation of GFA by back-transforming the PLS components to the original variables.

Results

A set of 22 molecules, shown in Table 1, whose stimulatory activities of adenylate cyclase were tested using the receptor surface model in the cockroach central nervous tissue, and whose Vmax values were 40% or larger than 40%, were selected as the target training set. The molecular structures and experimental biological activities are listed in Fig. 1a and Table 1, respectively. Vmax means the maximal response relative to octopamine and was expressed as the mean of 4 independent expreriments. Values of *pK*a (log of the reciprocal of *K*a) were used as octopamine-agonist activity index. *K*a is the concentration of octopamine agonist necessary for half-maximal activation of adenylate cyclase. The *K*a values were calculated from at least 5 concentrations ranging from 10^{-7} M to 10^{-3} M using a Macintosh personal computer system, and a sigmoidal curve-fitting program designed for log dose-probit activity analyses. 2-(2,6-Diethylphenylimino)imidazolidine **21** showed the highest activity followed by CAO **17**, OA **5** and 1-(2,6-diethylphenyl)imidazolidine-2-thione **18** in study compounds. The compounds **18** and **21** showed the almost same Vmax as octopamine, suggesting that only these compounds are full octopamine agonists and other compounds are partial octopamine agonists.

A receptor surface model was generated (Figs. 2 and 3)

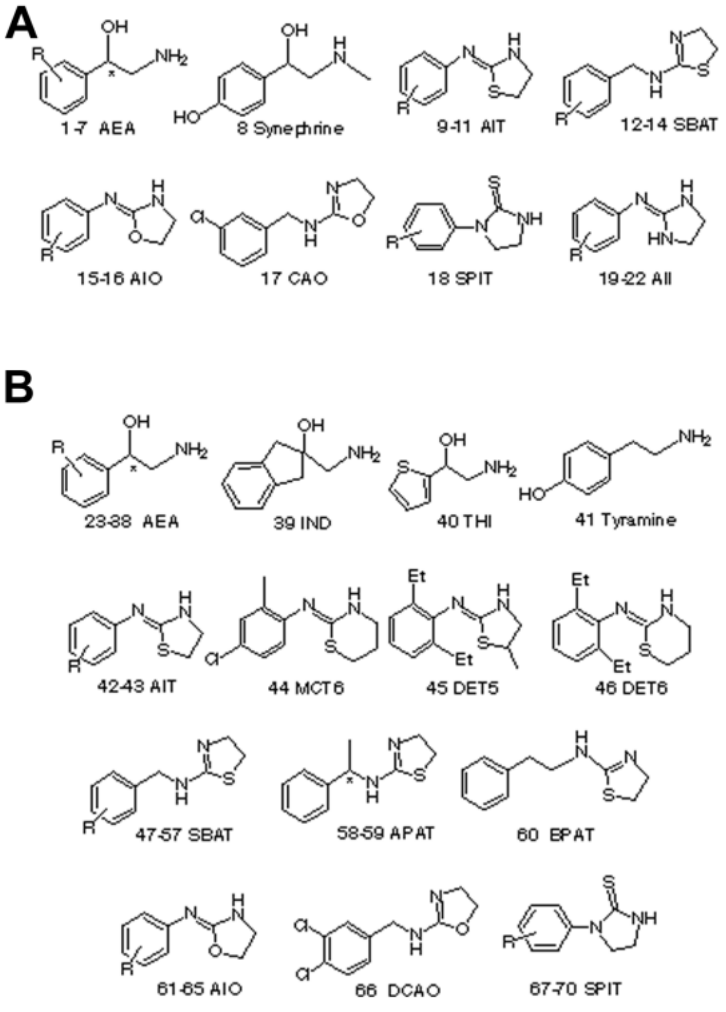

Figure 1. Structures of octopamine agonists used for regression analysis in study (a) and test (b) sets.

Table 1. Effect of OA agonists on the adenylate-cyclase activity in homogenates of American cockroach nerve cords in study set[a]

Compound				*pK*a		
no.	R	Vmax (%)	*K*a (μM)	Observed	Calculated[b]	Deviation[c]
			AAT			
1	2-MeO	45.8±3.2	1506.37 (1218.42-1871.21)	2.82	2.84	-0.02
2	4-Br	45.2±2.7	93.35 (84.46-103.29)	4.03	4.1	-0.07
3	4-Cl	72.1±1.2	68.77 (62.72-75.51)	4.16	3.93	0.23
4	4-F	44.0±0.9	273.39 (252.31-296.76)	3.56	3.69	-0.13
5	4-OH (OA)	100.0±5.5	6.58 (6.01-7.19)	5.18	5.01	0.17
6	4-Me	52.0±1.4	77.95 (67.32-90.41)	4.11	4.05	0.06
7	2,4-F_2	41.7±0.2	263.48 (235.45-295.11)	3.58	3.67	-0.09
			AIT			
8	Synephrine	57.6±5.6	150.03 (125.77-179.70)	3.82	3.9	-0.08
9	2-Me,4-Br	41.1±1.1	23.62 (20.19-27.83)	4.63	4.59	0.04
10	2,4-Me_2	55.0±3.9	13.65 (12.80-14.54)	4.86	4.85	0.01
11	2,6-Et_2	50.2±2.2	26.13 (25.04-27.26)	4.58	4.55	0.03
			SBAT			
12	3-F	40.8±1.5	35.04 (29.43-41.65)	4.46	4.31	0.15
13	3,4-Cl_2	52.5±6.2	17.51 (14.45-21.29)	4.76	4.73	0.03
14	3,5-Cl_2	45.7±4.6	16.25 (13.41-19.80)	4.79	5.15	-0.36
			AIO			
15	2,6-Et_2	57.9±1.8	16.84 (13.92-20.19)	4.77	4.83	-0.06
16	2-Et,6-*i* Pr	42.5±0.8	13.16 (10.39-16.54)	4.88	4.84	0.04
17	CAO	40.0±1.1	5.07 (4.12-6.14)	5.29	5.15	0.14
			SPIT			
18	2,6-Et_2	104.0±1.6	8.08 (6.32-10.26)	5.09	5.16	-0.07
			AII			
19	2,6-Me_2	47.7±7.6	15.03 (11.38-19.92)	4.82	4.88	-0.06
20	2-Me,6-Et	47.6±2.7	9.54 (7.48-12.10)	5.02	5.04	-0.02
21	2,6-Et_2	104.6±1.4	0.76 (0.49-1.13)	6.12	6.12	0
22	2,4,6-Me_3	59.1±10.2	8.40 (5.68-12.34)	5.08	5.06	0.02

[a]See the text for experimental details. The adenylate-cyclase activity of *P. americana* was measured according to Nathanson's procedure and the cAMP levels were measured by a RIA. Basal (control) and OA (100 μM)-stimulated (Vmax) adenylate cyclase activities were 116.2±5.4 and 1,473.3±59.3 pmol cAMP/min/mg of protein, respectively. In parentheses, 95% confidence limits are shown. *K*a and 95% confidence limit values were calculated with the Macintosh personal computer system using a sigmoidal curve-fitting program designed for log dose-probit activity analyses.

[b]Calculated by Equation (1).

[c]In case predicted activity is overestimated, deviation is obtained by calculating predicted activity subtracted by experimental value and indicated by minus. In case predicted activity is underestimated, deviation is obtained by calculating experimental activity subtracted by predicted value.

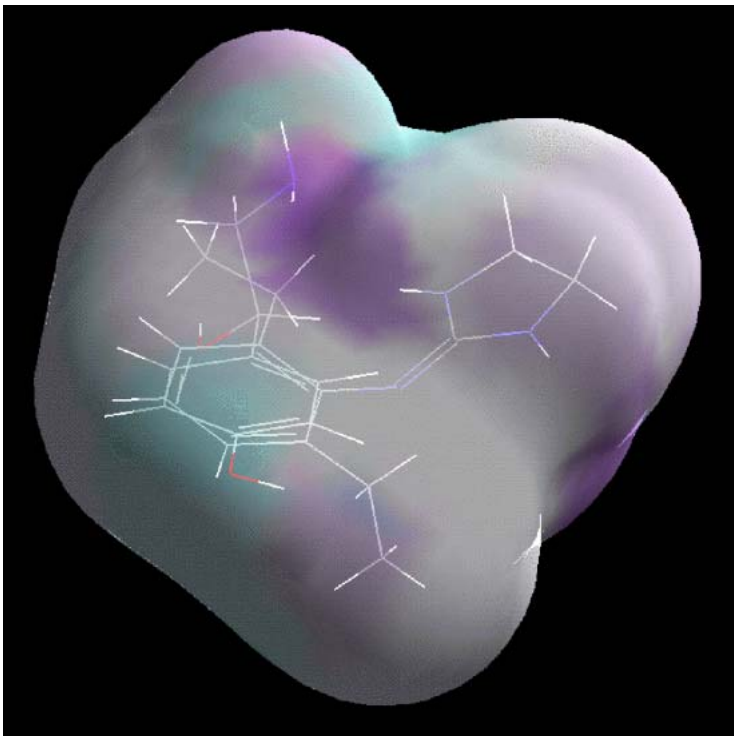

Figure 2. The octopamine agonist **21** with the highest activity and OA **5** embedded in an receptor surface model generated from **5**, **18** and **21** computed using the Wyvill steric function colored by H-bond contribution. The purple sign stands for a positive contribution of H-bond and a light-blue sign stands for a negative contribution of H-bond.

using same subset of the most active structures (**5**, **18** and **21**). The rationale underlying this model is that the most active structures tend to explore the best spatial and electronic interactions with

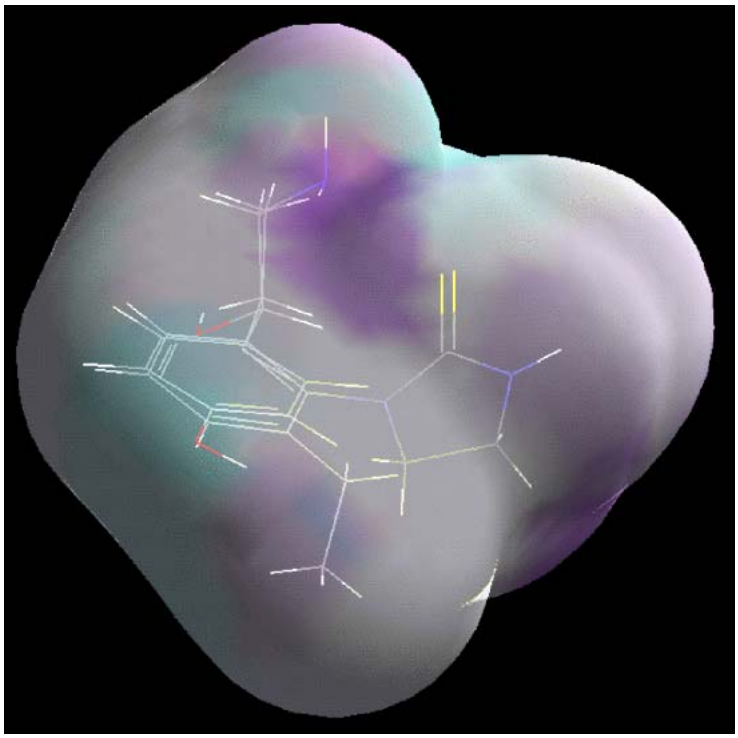

Figure 3. The octopamine agonist **18** and OA **5** embedded in an receptor surface model generated from **5**, **18** and **21** computed with the Wyvill steric function.

receptor, while the least active do not and tend to have unfavorable steric or electronic interactions. Fig. 2 shows octopamine agonist AII **21** with the highest activity and OA **5** embedded in a receptor surface model generated from the top 3 molecules. A rigid fit was performed to superimpose each structure so that it overlays the shape reference compound AII **21**. An ethyl group of **21** is superimposed with an aminoethanol side chain of **5**. The receptor surface model is colored by H-bond: a purple sign stands for a positive contribution of H-bond and a light-blue sign stands for a negative contribution of H-bond. The phenyl ring and 2,6-diethyl substituents have weak tendency to have an H-bond, while the nitrogen atom of **5** and one of nitrogen atom of imidazolidine in **21** share an area of strong H-bond contribution. The nitrogen atom of **5** actually serves as an H-bond acceptor (Hirashima *et al*., 2002a). The nitrogen atom of imidazolidine in **21** has a positive ionizable feature (Hirashima *et al*., 2002b), suggesting that it has a tendency to serve as an H-bond acceptor. The other nitrogen atom of **21** and the *p*-OH of **5** show a variable tendency to have an H-bond. Similarly, Fig. 3 shows another full octopamine agonist, SPIT **18**, and octopamine is embedded in a receptor surface model generated from the top 3 molecules. An ethyl group of **18** is superimposed on an aminoethanol side chain of **5**. The nitrogen atom of **5** and the sulfur atom of **18** share an area of strong H-bond contribution. The sulfur of **18** actually serves as an H-bond acceptor (Hirashima *et al*., 2002c). The 3-nitrogen atom of imidazolidine in **18** and *p*-OH of **5** have a variable tendency to have an H-bond.

The best model generated using the descriptors from the closed receptor surface model is given in Equation (1), which was statistically significant and used to correctly predict the activities of a set of training molecules ranging over 3 orders of magnitude (max. *pK*a 6.12 and min. *pK*a 2.82), indicating that these models could be useful tools to design active octopamine agonists. The energies of interaction between the receptor surface model and each molecular model were added to the study table as new columns, which were used for generating QSARs. Instead of one total number which is the sum of the interactions evaluated between each point on the surface and each molecular model, leading to one extra column in the study table, the energies at each surface point are available. Depending on the size of the drug molecules, this is potentially a great number of surface points. The number of variables for Equation (1) was 986. Ten percent of all new significant columns of variables were automatically used as independent X variables in the generation of QSAR. In order to quantitatively understand the dependence of biological activities on receptor surface model parameters of octopamine agonists, regression analysis was applied to representative 22 study compounds (Vmax $\geq$ 40%) listed in Fig. 1a and Table 1, leading to Equation (1).

$$pK\text{a} = 4.82948 + 2.46196(ELE/567 - 0.137016)^2 + 3.92126ELE/1565 - 1.19472ELE/1670 - 3.59779ELE/2177 + 3.86016ELE/3002 - 7.92195(VDW/678)^2 - 0.898844(VDW/1404 + 0.010941) - 3.36632(TOT/678)^2 - 1.68885(TOT/1866 + 0.243149) - 4.86016(TOT/2746 + 0.245914) - 2.94225(TOT/2746 + 0.114432) + 3.76445(TOT/2755 + 0.283752) + 4.13854(TOT/2755 + 0.267161) \quad (1)$$

where $n = 22$, $r^2 = 0.971$, $CV\text{-}r^2 = 0.720$, predicted sum of squares = 2.998 and $Bsr^2 = 0.968 \pm 0.001$. The descriptors *ELE/567*, *ELE/1565*

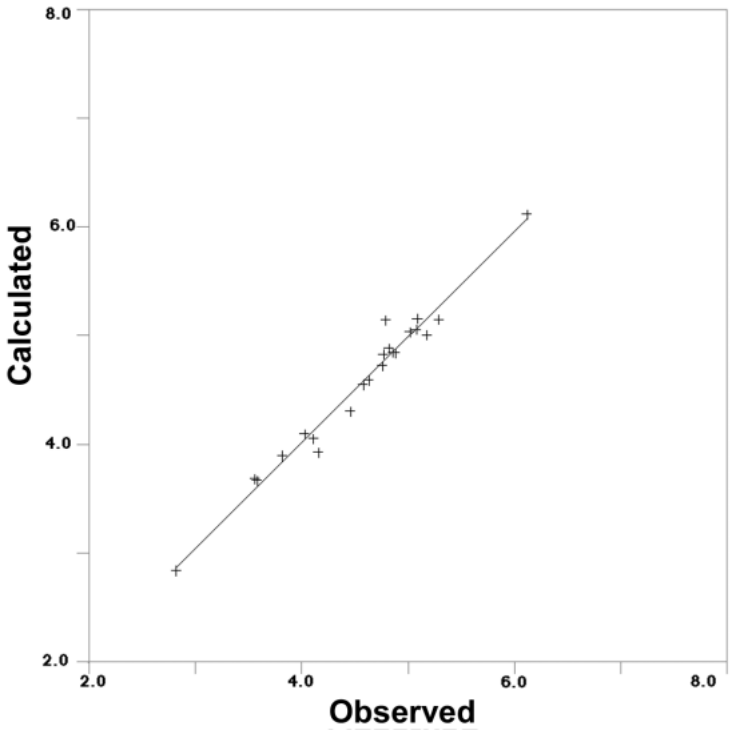

Figure 4. Correlation of observed *pK*a values with calculated *pK*a values from Table 1 using Equation (1) in study set.

etc are the electrostatic interaction energy of the molecule with the receptor at points 567, 1565 etc. The descriptors *VDW/678* and *VDW/1404* are the Van der Waals interaction energy of the molecule with the receptor at point 678 and 1404 etc. The descriptors *TOT/678*, *TOT/1866* etc are the added energy of both electrostatic interaction energy and Van der Waals interaction energy at point 678, 1866 etc. The term *n* means the number of data points; *r*-squared (r^2), the square of the correlation coefficient, which is used to describe the goodness of fit of the data of the study compounds to the QSAR model; cross-validated r^2 ($CV\text{-}r^2$), a squared correlation coefficient generated during a validation procedure using the equation: $CV\text{-}r^2$ = (SD - predicted sum of squares)/SD; SD, the sum of squared deviations of the dependent variable values from their mean; predicted sum of squares, the sum of overall compounds of the squared differences between the actual and the predicted values for the dependent variables. The predicted sum of squares value is computed during a validation procedure for the entire training set. The larger the predicted sum of squares value, the more reliable is the equation. A $CV\text{-}r^2$ is usually smaller than the overall r^2 for a QSAR equation. It is used as a diagnostic tool to evaluate the predictive power of an equation generated using the G/PLS method. Cross-validation is often used to determine how large a model (number of terms) can be used for a given data set. For instance, the number of components retained in G/PLS can be selected to be that which gives the highest $CV\text{-}r^2$. Bootstrap r^2 (Bsr^2) is the average squared correlation coefficient calculated during the validation procedure (Cerius2 tutorial, Accelrys Inc., www.accelrys.com/cerius2). A Bsr^2 is computed from the subset of variables used one-at-a-time for the validation procedure. It can be used more than one time in computing the r^2 statistic.

Table 1 depicts structures of octopamine agonists, their experimental *K*a values, calculated *pK*a values using Equation (1), and differences between observed and calculated *pK*a values. In case predicted activity is overestimated, deviation is obtained by calculating predicted activity subtracted by experimental value and indicated by a minus sign. In case predicted activity is underestimated, deviation is obtained by calculating experimental activity subtracted by predicted value. Residuals (observed versus calculated from Table 1) are plotted in Fig. 4.

Once the desired receptor surface model had been constructed, all the structures in the test sets were evaluated against the model. The evaluation consists of computing several energetic descriptors that are based upon the interactions between ligand and model. By using receptor data to develop a QSAR model, the goodness of fit can be evaluated between a candidate structure and a postulated pseudo-receptor. The predictive character of the QSARs was further assessed using test molecules, whose Vmax values are less than 40% and whose structures are shown in Fig. 1b, outside of the training set. The best statistically significant Equation (1) was applied to access these octopamine agonists. The predicted values of these molecules are listed in Table 2. The octopamine agonists showed reasonable predicted activities according to Equation (1) in intracellular cAMP production. Residuals (observed versus calculated from Table 2) are plotted in Fig. 5. These results may imply that the process of calculating a receptor surface model treats these structures reasonably, although they have low Vmax values.

Discussion

QSAR modeling is an area of research pioneered by Hansch and Fujita (1964), Hansch and Leo (1995), and Golender and Vorpagel (1993). QSAR attempts to model the activity of a series of compounds using measured or computed properties of the compounds. Receptor surface models are quantitative and differ from pharmacophore models, which are qualitative, in that the former

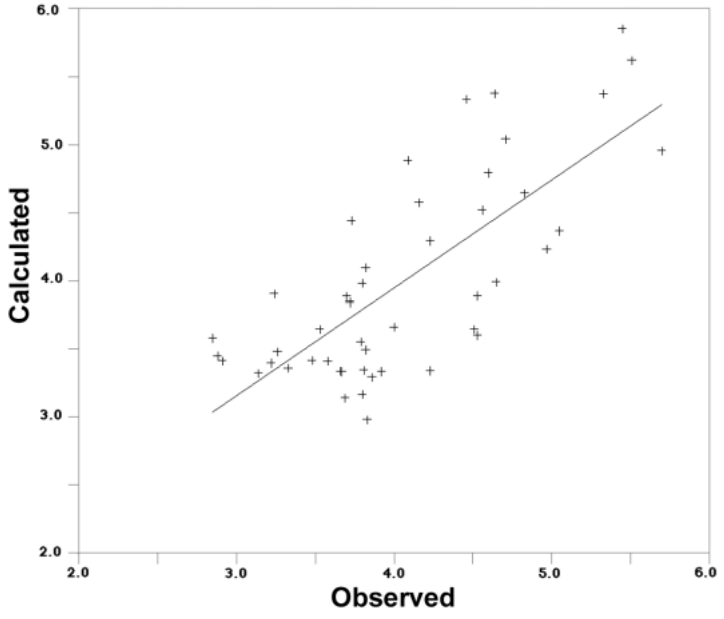

Figure 5. Correlation of observed *pK*a values with calculated *pK*a values from Table 2 using Equation (1) in test set.

Table 2. Effect of OA agonists on the adenylate-cyclase activity in homogenates of American cockroach nerve cords in test set[a]

Compound				*pK*a		
no.	R	Vmax (%)	*K*a (μM)	Observed	Calculated[b]	Deviation[c]
			AAT			
23	H (D)	34.2±1.1	215.24 (187.47-247.95)	3.67	3.34	0.33
24	H (L)	11.1±3.4	262.57 (193.61-344.80)	3.58	3.41	0.17
25	3-Br	13.4±0.9	154.00 (103.75-232.52)	3.81	3.35	0.46
26	3-Cl	19.0±0.6	157.63 (128.21-193.68)	3.8	3.99	-0.19
27	3-NO_2	19.2±0.2	407.55 (1083.37-1846.91	2.85	3.58	-0.73
28	4-NO_2	33.9±0	298.36 (280.53-317.65)	3.53	3.65	-0.12
29	4-CF_3	31.8±1.5	99.82 (87.32-114.29)	4	3.66	0.34
30	4-MeO	8.8±0.5	3.51 (2.52-4.88)	5.45	5.85	-0.4
31	4-MeS	25.9±1.5	1033.02 (859.05-1247.86	2.91	3.41	-0.5
32	4-Et	25.0±0.9	465.34 (387.24-556.93)	3.33	3.36	-0.03
33	2,3-Cl_2	15.6±0.9	137.24 (82.00-212.16)	3.86	3.3	-0.56
34	2,4-Cl_2	31.0±3.6	192.30 (165.79-223.06)	3.72	3.85	-0.13
35	2,4-Me_2	11.6±0.9	217.75 (109.38-449.32)	3.66	3.34	0.32
36	2,5-F_2	26.7±1.7	728.79 (585.31-921.35)	3.14	3.32	-0.18
37	2,6-$(MeO)_2$	16.6±0.4	555.13 (334.87-917.15)	3.26	3.48	-0.22
38	3,5-Cl_2	30.0±0.5	121.37 (98.43-149.89)	3.92	3.34	0.58
39	IND	13.8±0.8	581.64 (358.11-1025.27)	3.24	3.91	-0.67
40	THI	18.5±1.5	1328.80 (849.64-2218.85	2.88	3.45	-0.57
41	Tyramine	22.4±5.6	24.88 (19.65-31.28)	4.6	4.79	-0.19
			AIT			
42	2-Br,4-Me	25.0±2.5	148.39 (136.27-161.37)	3.83	2.98	0.85
43	2-Me,4-Cl	36.7±3.8	3.09 (2.06-4.82)	5.51	5.62	-0.11
44	MCT6	16.0±0.8	205.01 (144.37-280.93)	3.69	3.14	0.55
45	DET5	13.3±1.2	151.32 (119.24-191.64)	3.82	3.5	0.32
46	DET6	39.8±3.6	158.92 (130.35-193.83)	3.8	3.17	0.63
			SBAT			
47	H	20.9±1.0	29.51 (17.86-56.69)	4.53	3.6	0.93
48	2-Cl	24.3±1.5	192.02 (105.91-315.60)	3.72	3.84	-0.12
49	2-F	29.1±0.6	162.88 (122.07-230.02)	3.79	3.55	0.24
50	3-CF_3	26.1±3.3	69.55 (44.89-102.85)	4.16	4.58	-0.42
51	4-MeO	28.5±0.6	4.65 (3.06-6.99)	5.33	5.37	-0.04
52	2,4-Cl_2	34.3±0.9	27.55 (18.99-38.81)	4.56	4.52	0.04
53	2-F,4-Cl	29.2±1.9	22.63 (18.86-27.11)	4.65	3.99	0.66
54	2,5-Cl_2	27.9±2.2	8.91 (5.15-14.35)	5.05	4.37	0.68
55	2,6-$(MeO)_2$	8.1±0.6	59.09 (23.25-141.57)	4.23	3.34	0.89
56	3-Cl,4-F	12.3±0.7	10.74 (3.93-22.72)	4.97	4.24	0.73
57	3,4-F_2	19.3±2.9	80.36 (59.83-111.14)	4.09	4.89	-0.8
58	L-APAT	37.3±0.7	609.25 (552.91-672.55)	3.22	3.4	-0.18
59	D-APAT	16.0±1.2	328.60 (252.17-4321.21)	3.48	3.42	0.06
60	BPAT	22.7±0.6	185.65 (27.84-861.26)	3.73	4.44	-0.71
			AIO			
61	4-I	19.1±2.8	23.13 (17.18-31.01)	4.64	5.38	-0.74
62	2-Me,4-Br	33.9±2.3	19.54 (16.00-24.38)	4.71	5.04	-0.33
63	2,4-$(MeO)_2$	29.9±2.1	31.24 (16.26-56.13)	4.51	3.65	0.86
64	2,6-*i* Pr2	13.9±1.4	152.20 (100.57-219.87)	3.82	4.1	-0.28
65	2,3,4,5-Cl_4	27.0±2.0	29.68 (24.45-36.23)	4.53	3.89	0.64
66	DCAO	28.6±0.7	14.71 (11.47-18.77)	4.83	4.65	0.18
			SPIT			
67	2-Me,4-Cl	30.6±0.4	1.99 (1.61-2.47)	5.7	4.96	0.74
68	2,4-Me_2	10.5±0.5	34.64 (18.50-59.33)	4.46	5.34	-0.88
69	2-Me,5-Cl	10.8±0.7	201.47 (165.13-251.48)	3.7	3.89	-0.19
70	2,6-*i* Pr_2	23.8±0.3	59.49 (46.85-75.42)	4.23	4.29	-0.06

[a]See the text for experimental details. The adenylate-cyclase activity of *P. americana* was measured according to Nathanson's procedure and the cAMP levels were measured by a RIA. Basal (control) and OA (100 μM)-stimulated (Vmax) adenylate cyclase activities were 116.2±5.4 and 1,473.3±59.3 pmol cAMP/min/mg of protein, respectively. In parentheses, 95% confidence limits are shown. *K*a and 95% confidence limit values were calculated with the Macintosh personal computer system using a sigmoidal curve-fitting program designed for log dose-probit activity analyses.

[b]Calculated by Equation (1).

[c]In case predicted activity is overestimated, deviation is obtained by calculating predicted activity subtracted by experimental value and indicated by minus. In case predicted activity is underestimated, deviation is obtained by calculating experimental activity subtracted by predicted value.

tries to capture essential information about the receptor, while the latter only captures information about the commonality of compounds that bind. Receptor surface models tend to be geometrically overconstrained (and topologically neutral) since, in the absence of steric variation in a region, they assume the tightest steric surface that fits all training compounds. Receptor surface models do not contain atoms, but try to directly represent the essential features of an active site by assuming complementarity between the shape and properties of the receptor site and the set of binding compounds. The receptor surface model application uses 3D surfaces that define the shape of the receptor site by enclosing the most active members (after appropriate alignment) of a series of compounds. The global minimum of the most active compound **21** in the study compounds (based on the value in the activity column) was made as the active conformer. It really is just one of possibly many self-consistent models that fit the biological-activity data.

Octopamine is not likely to penetrate either the cuticle or the central nervous system of insects effectively, since it is fully ionized at physiological pH. Derivatization of the polar groups would be one possible solution to this problem in trying to develop potential pest-control agents. Generally speaking, antagonists are hydrophillic and they are not suitable for insecticides, because they can not penetrate through insect cuticle. Agonists also show higher binding affinity for the receptor (*pK*i: 9.54-3.92, Hirashima *et al*., 1999c) than antagonists (*pK*i: 8.99-4.09, Roeder, 1990). Therefore, it may be more applicable to develop agonists than antagonists as insecticides. Actually chlordimeform (*pK*i: 6.91, Roeder and Nathanson, 1993), whose active form *N*-demethylchlordimeform (*pK*i: 8.74) shows agonist activity (Nathanson and Hunnicutt, 1981), and Amitraz (*pK*i: 7.67) were developed as acaricides. Although AII **21** showed the highest activity both in octopamine agonist (*pK*a: 6.12) and binding (*pK*i: 9.54) activities, it showed no acaricidal activity, probably because it can not penetrate through insect cuticle, because SPITs **18** and **67**, which contain sulfur atom in the molecule, had acaricidal activity (Hirashima *et al*., 1992). Additionally, chlordimeform and **67** stimulated juvenile-hormone esterase followed by increase of ecdysteroids leading to delay of pupation in *Tribolium freemani* (Hirashima *et al*., 1998c). Furthermore, the octopamine agonists reported here inhibited calling behavior (Hirashima *et al*., 2003a) and *in vitro* pheromone synthesis of *Plodia interpunctella* (Hirashima *et al*., 2003b), whose action may be via a tyramine receptor (unpublished data), suggesting possible cross reactivity of those compounds with tyramine receptor.

There are several receptors that can be activated by octopamine in the central nervous system that can either activate or inhibit adenylyl cyclase activity (Brody and Cravchik, 2000). In addition, at least one of these receptors may be expressed in up to six alternatively spliced forms that may have different functional properties. Maximal stimulation of nerve cord adenylate-cyclase activity by **18**, **21** and **67** was inhibited by several antagonists, including mianserin, cyproheptadine, chlorpromazine and gramine (Hirashima *et al*., 1992). The rank-order ability of these antagonists to block the maximal adenylate cyclase activation by **18**, **21** and **67** was identical to the rank-order ability of the same antagonists to block the enzyme activation by an optimally effective concentration of octopamine. The β-adrenergic antagonist propranolol was less potent in this respect. Thus, the action of these octopamine agonists is same as that of octopamine, due to cAMP elevation at OAR2. The above receptor surface model studies show that full agonists with 2,6-diethyl substituents can be potential ligands to octopamine receptors. Phenyl ring-substitution requirements for partial octopamine agonists differ substantially from each other and other various types of octopamine agonists could be potent, although the type of compounds tested here are too limited to draw any conclusions. These derivatives could provide useful information in the characterization and differentiation of the octopaminergic receptor. They may help to point the way towards developing extremely potent, and relatively specific, octopamine ligands, leading to potential insecticides, although further research on the comparison of the 3D QSAR from agonists is necessary. In order to optimize the activities of these compounds as octopamine ligands, more detailed experiments are in progress.

Acknowledgements

This work was supported in part by a Grant-in-Aid for Scientific Research from the Ministry of Education, Science and Culture of Japan.

References

Axelrod J, Saavedra JM. 1977. Octopamine. *Nature* 265: 501-504.

Brody T, Cravchik A. 2002. *Drosophila melanogaster* G protein-coupled receptors. *Journal of Cell Biology* 150: 83-88.

Erspamer V, Boretti G. 1951. Identification and characterization by paper chromatography of enteramine, octopamine, tyramine, histamine, and allied substances in extracts of posterior salivary glands of Octopada and in other tissues of vertebrates and invertebrates. *Archives Internationales de Pharmacodynamie et de Therapie* 88: 296-332.

Evans PD. 1981. Multiple receptor types for octopamine in the locust. *Journal of Physiology* 318: 99-122.

Evans PD. 1985. Octopamine. In: Kerkut GA, Gilbert LI, editors. *Comprehensive Insect Physiology Biochemistry Pharmacology,* 11: 499-530. Oxford: Pergamon Press.

Evans PD. 1993. Molecular studies on insect octopamine receptors. In: Heller SR, editor. *Comparative Molecular Neurobiology*, 287-296. Basel: Birkhäuser Verlag.

Golender VE, Vorpagel ER. 1993. In: Kubinyi H, editor. *3D-QSAR in Drug Design: Theory, Methods, and Applications*:137. The Netherlands: ESCOM Science Publishers.

Hansch C, Fujita T. 1964. ρ-σ-π Analysis. A method for the correlation of biological activity and chemical structure. *Journal of American Chemical Society* 86: 1616-1626.

Hansch C, Leo A. 1995. In: *Exploring QSAR: Fundamentals and Applications in Chemistry and Biochemisry*. Washington, DC: American Chemical Society.

Hirashima A, Eiraku T, Shigeta Y, Kuwano E, Taniguchi E, Eto M. 2003b. Three-dimensional pharmacophore hypotheses of octopamine/tyramine agonists which inhibit [1-^{14}C]acetate incorporation in *Plodia interpunctella*. *Bioorganic and Medicinal Chemistry* 11: 95-103.

Hirashima A, Hirokado S, Tojikubo R, Takeya R, Taniguchi E, Eto M. 1998c. Metamorphosis of the red flour beetle, *Tribolium*

freemani Hinton (Coleoptera: Tenebrionidae): Alteration of octopamine content modulates activity of juvenile-hormone esterase, ecdysteroid level, and pupation. *Archives of Insect Biochemistry and Physiology* 37: 33-46.

Hirashima A, Morimoto M, Kuwano E, Taniguchi E, Eto M. 2002a. Three-dimensional common-feature hypotheses for octopamine agonist arylethanolamines. *Journal of Molecular Graphics and Modelling* 21: 81-87.

Hirashima A, Morimoto M, Kuwano E, Taniguchi E, Eto M. 2002b. Three-dimensional common-feature hypotheses for octopamine agonist 2-(arylimino)imidazolidines. *Bioorganic and Medicinal Chemistry* 10: 117-123.

Hirashima A, Morimoto M, Ohta H, Kuwano E, Taniguchi E, Eto M. 2002c. Three-dimensional common-feature hypotheses for octopamine agonist 1-arylimidazolidine-2-thiones. *Internet Journal of Molecular Science* 3: 56-68.

Hirashima A., Nagata T, Pan C, Kuwano E, Taniguchi E, Eto M. 1999c. Three dimensional molecular-field analyses of octopaminergic agonists and antagonists for the locust neuronal octopamine receptor (OAR3). *Journal of Molecular Graphics and Modelling* 17: 198-206.

Hirashima A, Pan C, E Kuwano, Taniguchi E, Eto M. 1999b. Three-dimensional pharmacophore hypotheses for the locust neuronal octopamine receptor (OAR3): 2. Agonists. *Bioorganic and Medicinal Chemistry* 7: 1437-1443.

Hirashima A, Pan C, Katafuchi Y, Taniguchi E, Eto M. 1996. Synthesis and octopaminergic-agonists activity of 2-(arylimino)oxazolidines and 2-(substituted benzylamino)-2-oxazolines. *Journal of Pesticide Science* 21: 419-424.

Hirashima A, Pan C, Tomita J, Kuwano E, Taniguchi E, Eto M. 1998a. Quantitative structure-activity studies of octopaminergic agonists and antagonists against nervous system of *Locusta migratoria*. *Bioorganic and Medicinal Chemistry* 6: 903-910.

Hirashima A, Shigeta Y, Eiraku T, Kuwano E. 2003a. Inhibitors of calling behavior of *Plodia interpunctella. Journal of Insect Science* 3: 4, http://insectscience.org/3.4/.

Hirashima A, Shinkai K, Kuwano E, Taniguchi E, Eto M. 1998b. Synthesis and octopaminergic-agonist activity of 3-(substituted phenyl)imidazolidine-2-thiones and related compounds. *Bioscience, Biotechnology and Biochemistry* 62: 1179-1184.

Hirashima A, Shinkai K, Pan C, Kuwano E, Taniguchi E, Eto M. 1999a. Quantitative structure-activity studies of octopaminergic ligands against *Locusta migratoria* and *Periplaneta americana*. *Pesticide Science* 55: 119-128.

Hirashima A, Tarui H, Eto M. 1994. Synthesis and octopaminergic-agonist activity of 2-(arylimino)thiazolidines, 2-(aralkylamino)-2-thiazolines, and related compounds. *Bioscience, Biotechnology and Biochemistry* 58: 1206-1209.

Hirashima A, Yoshii Y, Eto M. 1992. Action of 2-aryliminothiazolidines on octopamine-sensitive adenylate cyclase in the American cockroach nerve cord and on the two-spotted spider mite *Tetranycus urticae* Koch. *Pesticide Biochemistry and Physiology* 44: 101-107.

Hirashima A, Yoshii Y, Kumamoto K, Oyama K, Eto M. 1990. Structure-activity studies of insecticidal 2-methoxy-1,3,2-oxazaphospholidine 2-sulfides against *Musca domestica* and *Tribolium castaneum*. *Journal of Pesticide Science* 15: 539-551.

Ismail SMM, Baines RA, Downer RGH, Dekeyser MA. 1996. Dihydrooxadiazines: Octopaminergic system as a potential site of insecticidal action. *Pesticide Science* 46: 163-170.

Jennings KR, Kuhn DG, Kukel CF, Trotto SH, Whiteney WK. 1988. A biorationally synthesized octopaminergic insecticide: 2-(4-chloro-*o*-toluidino)-2-oxazoline. *Pesticide Biochemistry and Physiology* 30: 190-197.

Lowry OH, Rosebrough NJ, Farr AL, Randall RJ. 1951. Protein measurement with the Folin phenol reagent. *Journal of Biological Chemistry* 193: 265-275.

Nathanson JA. 1985. Phenyliminoimidazolidines. Characterization of a class of potent agonists of octopamine-sensitive adenylate cyclase and their use in understanding the pharmacology of octopamine receptors. *Molecular Pharmacology* 28: 254-268.

Nathanson JA, Hunnicutt EJ. 1981. *N*-Demethylchlordimeform: a potent partial agonist of octopamine-sensitive adenylate cyclase. *Molecular Pharmacology* 20: 68-75.

Nathanson JA, Kaugars G. 1989. A probe for octopamine receptors: synthesis of 2-[(4-azido-2,6-diethylphenyl)imino]imidazolidine and its tritiated derivative, a potent reversible-irreversible activator of octopamine-sensitive adenylate cyclase. *Journal of Medicinal Chemistry* 32: 1795-1799.

Pan C, Hirashima A, Kuwano E, Eto M. 1997b. Three-dimensional pharmacophore hypotheses for the locust neuronal octopamine receptor (OAR3): 1. Antagonists. *Journal of Molecular Modeling* 3: 455-463.

Pan C, Hirashima A, Tomita J, Kuwano E, Taniguchi E, Eto M. 1997a. *Internet Journal of Science-Biological Chemistry* 1: www.netsci-journal.com/97v1/97013/index.htm.

Roeder T. 1990. High-affinity antagonists of the locust neuronal octopamine receptor. *European Journal of Pharmacology* 191: 221-224.

Roeder T. 1992. A new octopamine receptor class in locust nervous tissue, the octopamine 3 (OA3) receptor. *Life Science* 50: 21-28.

Roeder T. 1995. Pharmacology of the octopamine receptor from locust central nervous tissue (OAR3). *British Journal of Pharmacology* 114: 210-216.

Roeder T, Gewecke M. 1990. Octopamine receptors in locust nervous tissue. *Biochemical Pharmacology* 39: 1793-1797.

Roeder T, Nathanson JA. 1993. Characterization of insect neuronal octopamine receptors (OA3 receptors). *Neurochemical Research* 18: 921-925.

Wu S-Y, Hirashima A, Takeya R, Eto M. 1989. Synthesis and insecticidal activity of optically active 2-methoxy-5-phenyl-1,3,2-oxazaphospholidine 2-sulfide. *Agricultural and Biological Chemistry* 53: 165-174.